Polarization effects in photoemission disentangle the origin of the shadow bands in Bi-based superconductors

M. Izquierdo,[1,2] J. Avila,[1,3] L. Roca,[1,3] G. Gu,[4] and M. C. Asensio[2,3]
[1]*LURE, Centre Universitaire Paris-Sud, Bât. 209D, B.P. 34, 91405 Orsay Cedex, France*
[2]*Synchrotron SOLEIL, L'Orme de Merisiers St Aubin, B.P. 48, 91192 Gif sur Yvette Cedex, France*
[3]*Instituto de Ciencia de Materiales, CSIC, 28049 Madrid, Spain*
[4]*Physics Department, Building 510B, Brookhaven National Laboratory, Upton, New York 11975-5000, USA*
(Received 27 May 2005; published 22 November 2005)

Angle-resolved photoemission spectroscopy has been used to investigate the origin of the shadow bands present at the Fermi surface of bismuth-based superconductors. Momentum distribution curves along the ΓY high-symmetry direction and Fermi surface maps measured on $Bi_2Sr_2CaCu_2O_{8+\delta}$ (Bi2212) single crystals with two different doping levels have revealed that the shadow bands and the main bands have different initial state symmetry. This result implies that the orthorhombicity exhibited by these materials cannot be responsible for their emergence at the Fermi surface.

DOI: 10.1103/PhysRevB.72.174517 PACS number(s): 74.72.Hs, 71.18.+y, 79.60.−i

The origin of the shadow bands (SB) at the Fermi surface of bismuth-based superconducting cuprates remains one of the unresolved questions regarding the electronic structure of these materials.[1] After their initial theoretical prediction[2] and first experimental obsevation,[3] two competing scenarios, antiferromagnetic correlations and structural distortions, have been supported theoretically and experimentally. From the theoretical side, the antiferromagnetic origin (AFO) has been sustained by correlation model calculations such as *stripe* models,[4,5] two-dimensional (2D) Hubbard model calculations at half filling,[6,7] or three-dimension (3D) Hubbard ones.[8] When doping is included in the 2D Hubbard model and within the weak coupling limit ($U<W$), SB appear as a consequence of the spin correlations,[2,9–11] although in some cases under conditions not fulfilled by the bismuth cuprates.[11] Similarly, *t-J* calculations have provided SB with an origin depending on the particular type of calculation.[12,13] On the other hand, in local-density approximation (LDA) band structure calculations,[14,15] SB only appear when the orthorhombicity of these materials[16] is taken into account. From an experimental point of view, photoemission (PE) experiments have tried to disentangle the origin of the SB either by comparing their behavior as a function of the binding energy with that of the main bands[17,18] or the intensity ratio of the shadow band and/or main band. In the former case, although initial results supported the AFO,[17] the latest measurements (with improved angular and energy resolution) are in favor of the structural distortion.[18] From an analysis of the intensity ratio, the orthorhombic distortion seems to be supported by the increasing of the SB intensity in Pb-doped Bi2212 compounds,[19,20] which have larger orthorhombic distortions, and the constant intensity ratio as a function of doping.[21,22]

Recent experiments have opened new perspectives. Thus, the observation that the intensity ratio shadow bands and/or main bands as a function of doping is not constant, but exhibits the same dependence as the superconducting transition temperature T_c, is in contradiction with the orthorhombic distortion and instead suggests that the SB are related to the superconductivity in these compounds.[25] Furthermore, we have recently shown the PE intensity ratio to be constant as a function of both the doping level and the number of CuO_2 planes,[22] which suggests a structural origin different from the orthorhombicity (which is larger in the Bi2201 compounds)[23], like a $c(2\times2)$ surface reconstruction.[24] These results would agree with VLEED experiments showing the presence of an intense $c(2\times2)$ diffraction, which are ascribed to a structural origin and would imply that extrinsic diffraction effects might have an important contribution to the SB.[26] The experiments performed so far have assumed that both SB and MB should have the same wave function since their Fermi surfaces have the same topology.[1] (See Fig. 1.)

In this paper, we have investigated the behavior of the SB as a function of the detection geometry in order to determine their initial state symmetry and shed some light onto their origin. ARPES measurements performed on Bi2212 single crystals with two different doping levels and detection geometries[22,27–29] have shown that, surprisingly, SB have a distinct initial state symmetry from that of the MB. This unexpected observation has allowed us to unambiguously rule out the scenario explaining their origin on the basis of the slight orthorhombic distortion present in these compounds or being an extrinsic effect due to final state diffraction.

The experiments were carried out at the Antares (SU8) beamline of LURE synchrotron in Orsay (France), details can be found elsewhere.[22,27–30] The main advantage of the experimental system is that the VSW hemispherical analyzer (acceptance angle 1°, energy resolution 50 meV) is mounted on a two-axis goniometer with a precision better than 0.5°, which allows constant polarization PE measurements (see Fig. 2). Two different symmetry detections are accessible: *even* and *odd*.[22,27–29] In both cases, the measurements are realized by keeping the sample fixed at a particular azimuthal angle (ϕ_M in Fig. 2) while the detector is moved. In the even detection mode, the configuration is such that the direction of the outgoing electrons ($\vec{k}_e$) is in the plane (ρ), defined by the

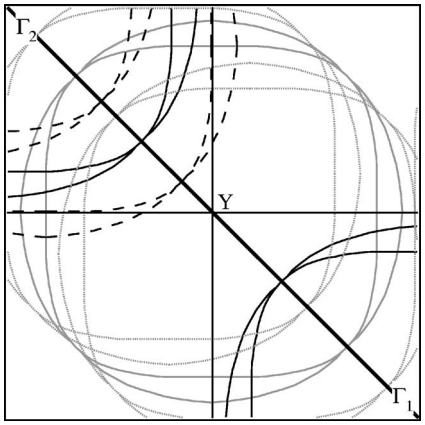

FIG. 1. Scheme representing the four quadrants of the Bi2212 tetragonal Brillouin zone sampled. Γ_1 corresponds to normal emission in our measurements and the line along $\Gamma_1 Y \Gamma_2$ corresponds to the measured polar scans. The theory for a two holelike FS adjusted from the measurements on an overdoped Bi2212 single crystal (Ref. 1) has been included as main bands (gray lines), their umklapps (dotted gray lines), shadow bands (black lines), and their umklapps (dashed black lines).

surface normal ($\vec{n}$), and the potential vector $\vec{A}$. Conversely, in the odd configuration, the direction of the outgoing electrons ($\vec{k}_e$) is not coplanar to the surface normal ($\vec{n}$) and the potential vector $\vec{A}$.

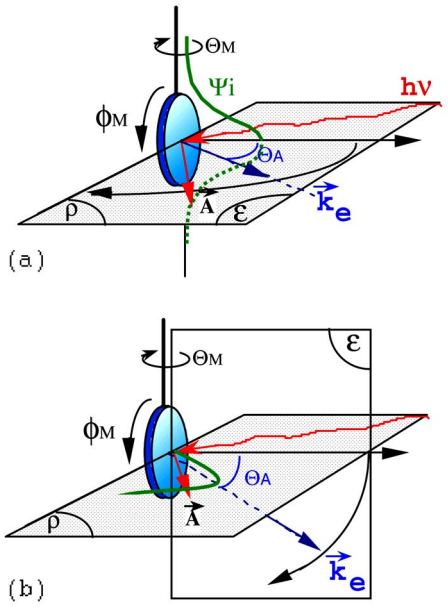

FIG. 2. (Color online) Experimental realization of the two geometry detection modes. (a) Even configuration: the direction of the outgoing electrons ($\vec{k}_e$) is in the plane (ρ) formed by the normal to the surface $\vec{n}$, and the potential vector $\vec{A}$. When measuring in a mirror plane of the sample, only even initial states will be detected. (b) Odd geometry: the direction of the outgoing electrons ($\vec{k}_e$) is in the plane (ε), perpendicular to that formed by $\vec{n}$ and ($\vec{A}$), therefore only odd initial states are accessible.

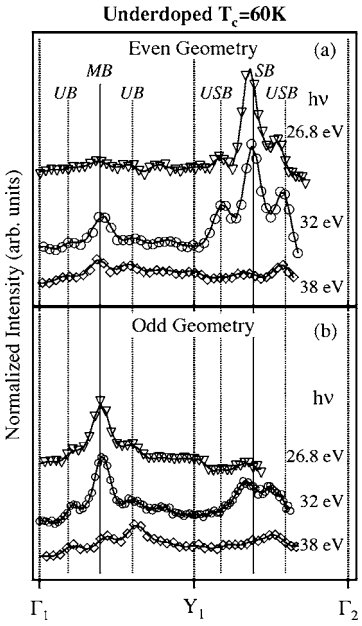

FIG. 3. Polar scans along the $\Gamma_1 Y \Gamma_2$ high-symmetry direction for photon energies $h\nu$=26.8, 32, and 38 eV in the even (a) and odd (b) detection geometries for the Bi2212 underdoped T_c=60 K sample. Vertical lines correspond to the position of the main band (MB), umklapp bands (UB), shadow bands (SB), and their umklapps (USB), respectively.

The influence of the photointensity on the two configurations can be understood by recalling the dipole matrix elements (ME) $\langle \psi_f | \vec{A} \cdot \vec{p} | \psi_i \rangle$. Since the total product $\psi_f \cdot \vec{A} \cdot \vec{p} \cdot \psi_i$ must be an even function in order to give a non-negligible photointensity, and the final function ψ_f must be even in order to be observed by the analyzer, we can infer that the final photointensity depends on the parity of the $\vec{A} \cdot \vec{p} \cdot \psi_i$ product. Thus, in the even (odd) detection configuration the product $\vec{A} \cdot \vec{p}$ is even (odd) and, therefore, in order to have a non-negligible photointensity the parity of the initial state ψ_i must be even (odd). In all measurements, $\vec{A}$ formed an angle of 45° with $\vec{n}$, mixed in-plane (s), and out-of-plane (p) polarizations. Since the orbitals at the Fermi level are essentially Cu $d_{x^2-y^2}$, O p_x, and p_y, the p part will not contribute to the photointensity. The samples investigated were high quality single Bi2212 crystals,[16] one at optimal doping (OD) (T_c=91 K) and the other underdoped (T_c=60 K) (U60). The samples were cleaved in an ultrahigh vacuum to obtain the high quality mirrorlike surfaces required for the experiment. An accurate *in situ* sample alignment was performed by high kinetic energy photoelectron diffraction of the Bi 5*d* core level, which allowed us to define the Γ point and the main high-symmetry directions. Two different types of measurements will be presented: momentum distribution curves along the $\Gamma_1 Y \Gamma_2$ high-symmetry direction (polar scans) and Fermi surface maps recorded as a series of polar scans for different azimuths of the samples to cover the selected regions of the reciprocal Brillouin zone.

Figure 3 displays the polar scans at the Fermi level along the $\Gamma_1 Y \Gamma_2$ high-symmetry direction for the U60 sample with the two available detection geometries. The $\Gamma_1 Y \Gamma_2$ has been

chosen because it is the highest symmetry direction of the material and therefore geometry detection effects will become dominant. Besides, along this direction the bands degenerate, thus they will cross the Fermi level at the same point and the results will be independent whether they are both holelike or one is electronlike at different doping levels (see Fig. 1). Moreover, the SB intensity along this direction has shown to be maximal.[22,31,32] In panel (a) of Fig. 3, the polar scans in the even detection geometry are presented for three different photon energies: $h\nu$=26.8, 32, and 38 eV. We observe that the maximum of intensity occurs in the second Brillouin zone at the position where the SB cross the Fermi level for $h\nu$=26.8 and 32 eV. Moreover, the high recorded photointensity for the SB in the second Brillouin zone contrasts with the low intensity for the MB in the first Brillouin zone. This behavior is more striking when compared with the results obtained for the odd detection geometry [panel (b)]. In this case, the situation is reversed from the previous one and the photointensity maximum occurs in the first Brillouin zone. This opposite behavior between the different detection geometries is indicative of a different initial state symmetry between the SB and the MB. In the case of $h\nu$=38 eV, we observe a large reduction of the overall intensity due to ME effects[27,29] and a similar intensity between the two Brillouin zones and detection geometries. This can be explained due to the contribution of the replicas[22] of the MB in the SB and vice versa. Considering they have different symmetry, the effect would be similar to a mixing of the symmetry, therefore a similar photointensity has been measured.

To confirm the different initial state symmetry and discard effects based only on the ME intensity differences, we have performed Fermi surface mappings covering the large section of the reciprocal space depicted in Fig. 1. Measurements were taken for the OD sample in the even detection geometry at $h\nu$=32 eV, conditions for which the photointensity of the SB becomes dominant in the second Brillouin zone. The result, displayed in Fig. 4, shows the photointensity to be symmetric with respect to the $\Gamma_1 Y \Gamma_2$. Furthermore, we can appreciate a very different behavior for the four measured quadrants, confirming the importance of the ME and their dependence on the Brillouin zone.[22,27–29] Concentrating on the two quadrants containing the $\Gamma_1 Y \Gamma_2$ high-symmetry direction, we see that the intensity coming from the main band vanishes in the first Brillouin zone along the $\Gamma_1 Y$ direction, which corresponds to the odd symmetry of the Cu $d_{x^2-y^2}$ orbitals with respect to this mirror plane. Conversely, in the second Brillouin zone, we observe that the maximum in photointensity appears around the $Y\Gamma_2$ direction at the crossing corresponding to the SB and their umklapps. This behavior of the intensity indicates that the SB do not have odd symmetry with respect to the $\Gamma_1 Y$ high-symmetry direction, otherwise the intensity would drop upon approaching it. The fact that the SB are almost invisible in the first Brillouin zone, in spite of their apparent even character, can be explained in terms of the relative orientation between the vector potential $\vec{A}$ and the direction of the momentum of the outgoing electrons $\vec{k}_e$, which in the first Brillouin zone is almost perpendicular, and therefore the resulting ME has a much reduced intensity. It also accounts for both the drop of

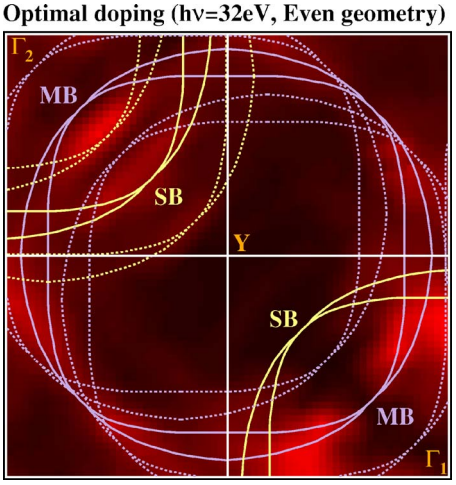

FIG. 4. (Color online) Fermi surface map of a Bi2212 sample measured at $h\nu$=32 eV in the even detection geometry for the Brillouin zone region depicted in Fig. 1. The theoretically expected Fermi surface has been included for both SB (MB) yellow (purple) solid lines and their respective umklapps bands as dashed yellow (purple) lines.

intensity when going from the first to the second Brillouin zone[27,29] and the reduction of the photointensity from the MB and their umklapps in the second Brillouin zone observed in Fig. 4.

In Fig. 5, a portion of the Fermi surface in the first Brillouin zone measured at $h\nu$=32 eV in the odd geometry detection for the OD sample is presented. This configuration has the advantage of an $\vec{A}$ that is not coplanar with $\vec{k}_e$, thus the MB and SB should have a similar intensity due to the ME effects in the first Brillouin zone. Indeed, we can observe that there is photointensity for both the SB and the MB with a comparable magnitude. Regarding the main band, we see a maximum of intensity around the $\Gamma_1 Y$ direction and a reduc-

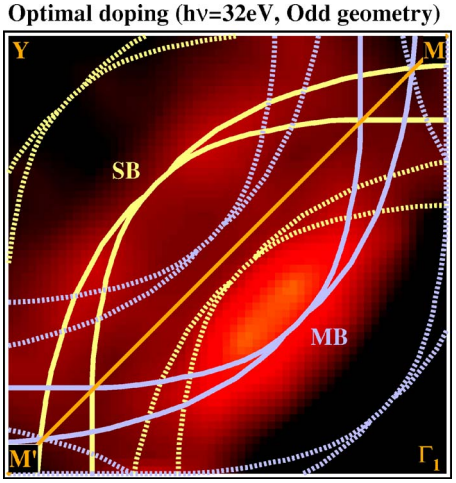

FIG. 5. (Color online) Photointensity map of a quadrant of the first Brillouin zone Fermi surface of the optimally doped Bi2212 sample measured at $h\nu$=32 eV in the odd detection geometry. The theoretical Fermi surface has been included using the same line criteria as in Fig. 4.

tion upon separation from this high-symmetry direction. On the contrary, for the SB we observe that the photointensity has a minimum along the $\Gamma_1 Y$ high-symmetry direction and it increases as we go away from it. However, in contrast to the even situation, they are very clearly detected outside the Γ_1Y direction.

This behavior confirms the result obtained from the analysis of Fig. 4: the SB and the main bands have different initial state symmetry. This observation has extremely important consequences for the interpretation of the origin of the SB. In particular, it rules out the orthorhombic scenario because, in this case, SB and MB are the same bands in two different orthorhombic Brillouin zones and they would have the same wave function, and consequently identical initial state symmetry. This observation is also inconsistent with the recently proposed interpretation which described the SB to final state extrinsic effects as due to final-state diffraction observed by VLEED,[26] which seemed to be consistent with our previous observation of the constant SB and/or MB intensity as a function of both the doping and the number of planes.[22] Since the wealth of experimental data[18–21,25] does not support the AFO scenario either, the topic of the origin of the SB is newly open, a plausible explanation being the initially proposed $c(2\times2)$ surface reconstruction[24] whose diffraction spots would be those observed by VLEED.[26]

In summary, we have performed a study of the shadow band initial state symmetry in Bi2212 superconductors. The polar scans measured along the $\Gamma_1 Y \Gamma_2$ for an underdoped T_c=60 K sample have indicated a different initial state symmetry between the main and the shadow bands in these materials, which has been confirmed by Fermi surface mappings of the Bi2212 sample at optimal doping. This observation is crucial because the different symmetry indicates that shadow bands are an initial state effect, thus discarding the origin of the shadow bands based on extrinsic effects due to final-state diffraction. Furthermore, this observation also rules out the orthorhombic scenario. We conclude that, in spite of the slight orthorhombic distortion present in these materials, electrons moving at the Fermi energy see a tetragonal Brillouin zone.

The authors thank A. Bansil, M. Lindroos, and A. Santander for the interesting discussions. This work has been financed by the Spanish MCYT project MAT2002-0343 and the Large-Scale Installation Program at LURE under Grant No. HPRI-CT-1999-00034. M.I. and L.R. thank Spanish MCYT for their support.

[1] A. Damascelli, Z.-X. Shen, and Z Hussain, Rev. Mod. Phys. **75**, 473 (2003).
[2] A. P. Kampf and J. R. Schrieffer, Phys. Rev. B **41**, 6399 (1990); *ibid.* **42**, 7967 (1990).
[3] P. Aebi, J. Osterwalder, P. Schwaller, L. Schlapbach, M. Shimoda, T. Mochiku, and K. Kadowaki, Phys. Rev. Lett. **72**, 2757 (1994).
[4] M. Moraghebi, C. Buhler, S. Yunoki, and A. Moreo, Phys. Rev. B **63**, 214513 (2001).
[5] M. I. Salkola, V. J. Emery, and S. A. Kivelson, Phys. Rev. Lett. **77**, 155 (1996).
[6] S. Onoda and M. Imada, Phys. Rev. B **67**, 161102(R) (2003).
[7] F. F. Assaad and M. Imada, Eur. Phys. J. B **10**, 595 (1999).
[8] S. Grabowski, J. Schmalian, and K. H. Bennermann, Solid State Commun. **102**, 493 (1997).
[9] A. V. Chubukov, Phys. Rev. B **52**, R3840 (1995).
[10] S. Haas, A. Moreo, and E. Dagotto, Phys. Rev. Lett. **74**, 4281 (1995).
[11] Y. M. Vilk, Phys. Rev. B **55**, 3870 (1997).
[12] M. F. Bishop, Z. P. Gibbs, and T. McMullen, Phys. Rev. B **59**, 14937 (1999).
[13] R. Eder and Y. Ohta, Phys. Rev. B **56**, 2542 (1997).
[14] D. J. Singh and W. E. Pickett, J. Supercond. **8**, 583 (1995); Phys. Rev. B **51**, 3128 (1995).
[15] W. E Pickett, Rev. Mod. Phys. **61**, 433 (1989).
[16] G. Gu, K. Takamuku, N. Koshizuka, and S. Tanaka, J. Cryst. Growth **130**, 325 (1993).
[17] S. LaRosa, R. J. Kelley, C. Kendziora, G. Margaritondo, M. Onellion, and A. Chubukov, Solid State Commun. **104**, 459 (1997).
[18] A. Koitzsch, S. V. Borisenko, A. A. Kordyuk, T. K. Kim, M. Knupfer, J. Fink, M. S. Golden, W. Koops, H. Berger, B. Keimer, C. T. Lin, S. Ono, Y. Ando, and R. Follath, Phys. Rev. B **69**, 220505 (2004)(R).
[19] P. Aebi, J. Osterwalder, P. Schwaller, H. Berger, C. Beeli, and L. Schlapbach, J. Phys. Chem. Solids **56**, 1845 (1995).
[20] P. Schwaller, P. Aebi, H. Berger, C. Beeli, J. Osterwalder, and L. Schlapbach, J. Electron Spectrosc. Relat. Phenom. **76**, 127 (1995).
[21] P. Schwaller, T. Greber, P. Aebi, J. M. Singer, H. Berger, L. Forró, and J. Osterwalder, Eur. Phys. J. B **18**, 215 (2000).
[22] M. Izquierdo, Ph.D. thesis, Universidad Autóma Madrid, 2003; M. Izquierdo *et al.* (unpublished).
[23] C. C. Torardi, M. A. Subramanian, J. C. Calabrese, J. Gopalakrishnan, E. M. McCarron, K. J. Morrisey, T. R. Askew, R. B. Flippen, U. Chowdry, and A. W. Sleight, Phys. Rev. B **38**, 225 (1988).
[24] S. Chakravarty, Phys. Rev. Lett. **74**, 1885 (1995).
[25] A. A. Kordyuk, S. V. Borisenko, M. S. Golden, S. Legner, K. A. Nenkov, M. Knupfer, J. Fink, H. Berger, L. Forró, and R. Follath, Phys. Rev. B **66**, 014502 (2002).
[26] V. N. Strocov, R. Claessen, and P. Blaha, Phys. Rev. B **68**, 144509 (2003).
[27] M. C. Asensio, J. Avila, L. Roca, A. Tejeda, G. D. Gu, M. Lindroos, R. S. Markiewicz, and A. Bansil, Phys. Rev. B **67**, 014519 (2003).
[28] L. Roca, M. Izquierdo, A. Tejeda, D. G. Gu, J. Avila, and M. C. Asensio, Appl. Surf. Sci. **212–213**, 62 (2003).
[29] A. Bansil, M. Lindroos, S. Sahrakorpi, R. S. Markiewicz, G. D. Gu, J. Avila, L. Roca, A. Tejeda, and M. C. Asensio, J. Phys. Chem. Solids **63**, 2175 (2002).
[30] M. E. Dávila, S. L. Molodtsov, M. C. Asensio, and C. Laubschat,

Phys. Rev. B **62**, 1635 (2000).
[31] N. L. Saini, J. Avila, A. Biaconi, A. Lanzara, M. C. Asensio, S. Tajima, G. D. Gu, and N. Koshizuka, Phys. Rev. Lett. **79**, 3467 (1997).
[32] A. Bianconi, N. L. Saini, A. Valletta, A. Lanzara, J. Avila, M. C. Asensio, S. Tajima, G. D. Gu, and N. Koshizuka, J. Phys. Chem. Solids **59**, 1884 (1998).